Journal of Biomedical Optics 6(3), 371–377 (July 2001)

Design of synchrotron light source and its beamline dedicated to dual-energy x-ray computed tomography

Masami Torikoshi
Takanori Tsunoo
Masahiro Endo
Koji Noda
Masayuki Kumada
Satoru Yamada
Fuminori Soga
National Institute of Radiological Sciences
Anagawa 4-9-1
Inage
Chiba 263-8555, Japan

Kazuyuki Hyodo
High Energy Accelerator Research Organization
Oho 1-1
Tsukuba 305-0801, Japan

Abstract. A synchrotron light source dedicated to medical applications has been designed at National Institute of Radiological Sciences. The storage ring, with circumference of 80 m, is designed for acceleration of 2.3 GeV and a stored current of 420 mA. It is equipped with two multipole wigglers to produce sufficient photon flux in a hard x-ray region required for medical applications. The purposes of the synchrotron light source are clinical performance of medical diagnoses clinically and research and development relating with medical applications. One of the most interesting applications for us is dual-energy x-ray computed tomography (CT). It gives the information about electron density of human tissue. The information plays an important role in advancing heavy-ion radiotherapy of cancers. Electron density can be derived from attenuation coefficients measured by different energy x rays. In this paper, a practical method of the dual-energy x-ray CT with synchrotron radiation is proposed with the theoretical consideration. The primitive experiment using monochromatic x rays emitted from radioisotopes proved the procedure of analysis mentioned here effective to derive electron densities from linear attenuation coefficients for two x rays of a different energy. The beamline dedicated to dual-energy x-ray CT is also proposed. It has a multipole wiggler as a light source and it mainly consists of a dual crystal monochromator and a rotating filter for attenuating photon flux of x rays and two-dimensional detector. [DOI: 10.1117/1.1383062]

Keywords: x-ray computed tomography; synchrotron radiation; monochromatic x ray; electron density.

Paper JBO-014103 received June 19, 2000; revised manuscript received Jan. 23, 2001; accepted for publication Feb. 27, 2001.

1 Introduction

Synchrotron radiation (SR) has great advantages for advancing x-ray imaging and medical diagnoses. We have a plan to construct a compact synchrotron light source dedicated to medical applications at the National Institute of Radiological Sciences (NIRS). The final goal of our plan is: (1) construction of the compact light source based on a hospital and (2) clinical uses of advanced medical diagnoses with SR. A typical medical application of synchrotron radiation is intravenous coronary angiography (CAG).[1] It has been clinically applied to examinees as a noninvasive diagnostic method for discovering coronary heart disease.[2–4] In addition, there are many other applications of synchrotron radiation, such as monochromatic x-ray computed tomography, fluorescent x-ray imaging, noninvasive bronchography, phase contrast imaging, refraction contrast imaging, and so forth. These help discover diseases at an early stage and determine optimum treatments for the diseases.

Our plan is motivated by heavy-ion radiotherapy, which has been performed with carbon beams at the NIRS since 1994.[5,6] More precise heavy-ion irradiation can be achieved with the help of computed tomography (CT) with monochromatic x rays. CT with monochromatic x rays provides information about electron density of human tissue without ambiguity due to the beam hardening effect. The information makes the planning of the treatment of heavy-ion radiotherapy more accurate. Electron density is also expected to introduce new information into medical diagnosis. In order to measure electron density of human tissue, study of dual-energy x-ray CT was begun using conventional CT scanners in the 1970s.[7] Dilmanian et al. have been developing dual-energy x-ray CT with SR to separate the concentration of low-Z elements and that of intermediate-Z elements. The latter concentration provides the information on important elements for human tissues such as Potassium.[8]

We designed the synchrotron light source dedicated to medical applications. One of the beamlines of the synchrotron light source is designed for performing dual-energy x-ray CT clinically for patients with lesions in their brains. In this paper, we focus on a basic concept of dual-energy x-ray CT and design of the beamline as well. The design of the synchrotron light source is also introduced briefly.

Address all correspondence to Masami Torikoshi. Tel: 81-43-251-2111(Ext. 6872); Fax: 81-43-251-1840; E-mail: torikosi@nirs.go.jp

1083-3668/2001/$15.00 © 2001 SPIE

2 Dual-Energy X-Ray CT

2.1 Basic Concept

Employing a formula proposed by Jackson and Hawkes,[9] a linear attenuation coefficient of a matter for an x-ray of an energy E is described as follows:

$$\mu=\frac{\rho N_A}{A}\left[4\sqrt{2}Z^5\alpha^4\left(\frac{mc^2}{E}\right)^{3.5}\phi_0\sum_{nll'}f_{nll'}+Z_e\sigma^{KN}+(1-Z^{b-1})\left(\frac{Z}{Z'}\right)^2\sigma^{coh}(Z',E')\right], \tag{1}$$

where ρ, N_A, A, and Z are density, Avogadro's number, an atomic mass, and an atomic number, respectively. The first term in a parenthesis is an atomic cross section of photoelectric absorption. Description for the photoelectric absorption cross section involves L-shell electrons as well as K-shell electrons. An incoherent cross section for an atom with Z is described by the sum of a Klein–Nishina cross section multiplied by Z and a correction term, which is described by a coherent cross section multiplied by minus Z^{b-1}. A coherent cross section can be related to the coherent cross section for a standard element Z'. Here, we used the element with $Z'=8$, oxygen, as the standard element. Equation (1) can be simplified as follows for convenience:

$$\mu=\rho_e[Z^4F(E,Z)+G(E,Z)], \tag{2}$$

where $\rho_e=(\rho N_A/A)Z$ is electron density, and the first term and the second term in the parenthesis denote a photoelectric absorption term and a photon scattering term, respectively. There are two unknown variables: ρ_e and Z.

Using a light source with an energy spectrum in which discrete two peaks of energy E_1 and E_2 exist, transmitted lights through an object are simply described as follows:

$$\begin{aligned}I_A&=I_{1A}\exp\left(-\int\mu(E_1,x)dx\right)+I_{2A}\exp\left(-\int\mu(E_2,x)dx\right),\\ I_B&=I_{1B}\exp\left(-\int\mu(E_1,x)dx\right)+I_{2B}\exp\left(-\int\mu(E_2,x)dx\right),\end{aligned} \tag{3}$$

where indices A and B denote different energy spectra. I_1 and I_2 are incident x-ray intensities of energy E_1 and E_2, respectively. The incident x-ray intensities can be easily measured in combination of dosimetry and pulse-height analysis. Solving the simultaneous equations derives exponential functions of integration of a linear attenuation coefficient. In CT reconstruction algorithms, numeric values of $\mu(E_1)$ and $\mu(E_2)$ for each pixel can be obtained. Then, using Eq. (2), we obtain other simultaneous equations with respect to the linear attenuation coefficients as follows:

$$\mu_1=\rho_e[Z^4F(E_1,Z)+G(E_1,Z)],$$

$$\mu_2=\rho_e[Z^4F(E_2,Z)+G(E_2,Z)].$$

The linear attenuation coefficient for elements of human tissue is approximately proportional to Z^4. In order to obtain Z, we can solve the simultaneous equations with respect to Z^4 as follows:

$$Z^4=\frac{\mu(E_2)G(E_1,Z)-\mu(E_2)G(E_1,Z)}{\mu(E_1,Z)F(E_2,Z)-\mu(E_2,Z)F(E_1,Z)}. \tag{4}$$

Iterative calculation results in a unique solution of Z. We call the Z an effective atomic number. Then we can easily obtain electron density with the following equation using the effective atomic number Z:

$$\rho_e=\frac{\mu(E_1)F(E_2,Z)-\mu(E_2)F(E_1,Z)}{F(E_2,Z)G(E_1,Z)-F(E_1,Z)G(E_2,Z)}. \tag{5}$$

Two-dimensional (2D) mapping of linear attenuation coefficients of an object or CT numbers is reconstructed as a CT image in a conventional x-ray CT. In the dual-energy x-ray CT, 2D mapping of ρ_e or Z of an object is obtained. Experiments using monochromatic x rays emitted from radioisotopes partially proved the effectiveness of Eqs. (4) and (5), and those results were presented in Sec. 2.4.

As shown in the simultaneous equations (3), there are two types of x-ray beams. One type of x-ray beam contains an x-ray of energy E_1 and that of E_2 with a flux ratio of $I_{1A}:I_{2A}$. The other type contains both the x-ray beams with ratio of $I_{1B}:I_{2B}$. These beams are easily produced with a combination of a monochromator and filters of two kinds as mentioned in the next subsection.

2.2 Design of Beamline for Dual-Energy X-ray CT

We propose the beamline dedicated to the dual-energy x-ray CT for clinical uses. Figure 1 shows the beamline schematically. The light source of the beamline is a multipole wiggler mentioned later. The beamline length from the center of the light source to a detector is about 15 m. Main components of the beamline are a monochromator, a rotating filter, collimators, a beam shutter, dose meters, a beam stopper, and so forth. The components except for the first two are generally used in a synchrotron radiation beamline. The monochromator consists of dual silicon crystal with (220) surface. The Si(220) crystal plane reflects the second order harmonic wave parasitically as well as the first order harmonic wave. Since the wiggler provides us with sufficient photon flux of the higher energy region than about 80 keV, which is shown in Figure 4, we can use the first and second order harmonic waves simultaneously as the dual-energy x ray. Then, energy E_2 in Eq. (3) is twice as large as E_1. Using only different filters gives a change in the ratio of photon flux of the first order harmonic wave to that of the second one; that is $I_{1A}/I_{2A}\neq I_{1B}/I_{2B}$, where the indices of A and B denote the different filters. For each projection in CT scanning, two transmission images are taken by inserting both the filters one after the other into the beamline. Figure 2 shows it schematically. Both the filters are combined in the rotating filter shown in the figure. A part of the rotating filter is made of metal such as copper, and another part is made of a lighter material such as graphite. The rotating filter is located upstream of the monochromator so that it

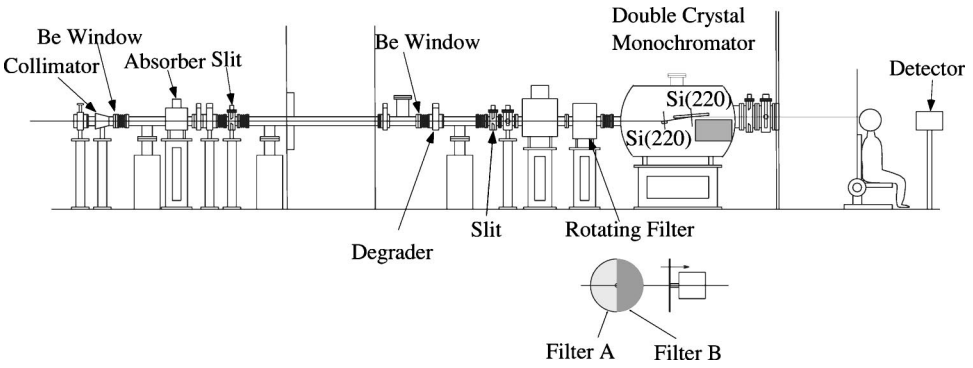

Fig. 1 A schematic drawing of the beamline used for the dual-energy x-ray CT. In this design, the target is limited to a head of an examinee. The examinee is rotated in a rate of 180°/20–30 s when being exposed to x rays. Rotating two different filters alternatively changes relative amounts of the first and second order harmonic waves.

receives the white light and decreases the heat load in the monochromator. The heavier part of the filter strongly attenuates a low energy part of the synchrotron radiation, and the lighter part does not modify the energy spectrum very much but reduces the intensity of the photon flux.

The second crystal located downstream of the first one has an asymmetry reflection surface to expand the x-ray beam vertically[10] in order to make the irradiation field of $V50\,\mathrm{mm} \times H300\,\mathrm{mm}$ at the examinee's position. The magnification of the vertical size is given by the following equation:

$$M = \frac{\sin(\theta_B + \alpha)}{\sin(\theta_B - \alpha)} \approx \frac{\theta_B + \alpha}{\theta_B - \alpha}, \tag{6}$$

where M is the magnification, θ_B is a Bragg angle for the first order harmonic wave, and an asymmetry angle α is the angle between the (220) plane and the surface of the crystal. The incident angle of an x ray onto the crystal surface is $\theta_B - \alpha$. The small incident angle of $\theta_B - \alpha$ makes the longitudinal size of the second crystal larger than that of the first crystal in order to cover the whole vertical size of the SR beam with a fan shape.

For CT scan with SR, an examinee is put into rotation instead of an x-ray source. Since the beam of SR is parallel, a rotation of from 0° to only 180° is sufficient for a scan.[11] Considering about 800 projections are taken in a conventional CT scan over 360°, 400 projections are supposed to be sufficient for reconstruction of a tomographic image. It is necessary to rotate an examinee in a slow rate such as from 20 to 30 s for 180° so as to prevent the examinee from moving from one's original position. Even the slight motion may cause artifacts in reconstruction images. Even though the rotation is slow, it is required that the exposure time to take each transmission image and an interval time between those exposures for a projection be as short as from a few milliseconds to tens of milliseconds so as to make a reconstruction image free from artifact due to the rotation.

Use of a two-dimensional detector can take transmission images for multislices simultaneously so that it shortens the total scanning time. Recently a flat-panel detector has been used for computed radiography (CR).[12] The important condition required for the detector for our purpose is a higher frame rate than a video rate of 30 frame/s. Nakagawa and his colleagues have been developing complimentary metal–oxide–semiconductor (C-MOS) arrays to realize real time imaging.[13] A C-MOS device can transfer in principle a larger electric charge than usually used with devices such as a charge-coupled device. Therefore a large area C-MOS sensor can be produced. It is suitable from a standpoint of radiation safety

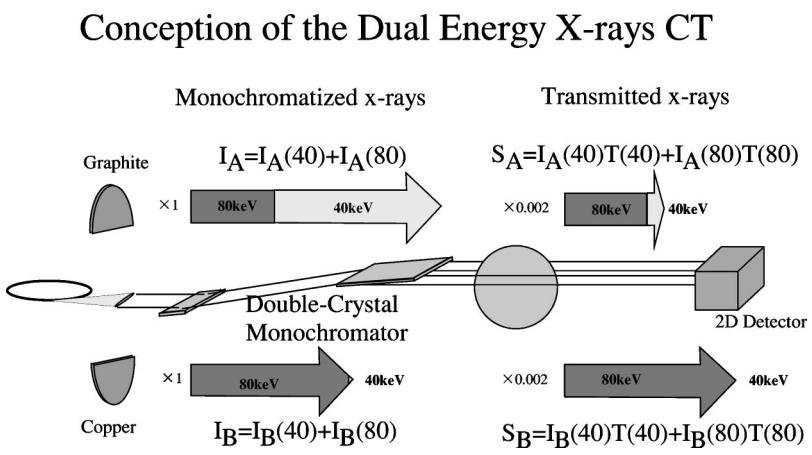

Fig. 2 A schematic drawing to explain the concept of the dual-energy x-ray CT.

Table 1 Photon flux estimation for dual-energy x-ray CT.

	40 keV		80 keV	
Total photon flux in front of a filter (ph/sec)[a]	1.88×10^{14}		4.92×10^{13}	
Specification of filter	Graphite (13 g/cm^2)		Copper (1.8 g/cm^2)	
	40 keV	80 keV	40 keV	80 keV
Photon flux in front of an object (photons/sec)	1.27×10^{13}	5.44×10^{12}	3.40×10^{10}	1.28×10^{13}
Ratio of photon flux of 40 keV to that of 80 keV	2.34		0.003	
Radiation dose (mGy) [Surface dose (mSv)[b]]	10 [14]			
Photon flux per pixel[c] in absence of an object	6.05×10^{6}		4.26×10^{6}	
Photon flux per pixel in presence of an object[d]	8.78×10^{3}		1.73×10^{4}	

[a] A radiation field size is assumed to be 5 cm×30 cm.

[b] Conversion coefficients for skin dose of AP were quoted from ICRP Publication 51, 1987.

[c] Pixel size is 1 mm×10 mm.

[d] An object is assumed to have a water equivalent length of 30 cm.

that a pixel size is 1 mm×10 mm, which is the same as that used in a conventional CT scanner. Besides, since a C-MOS device can make faster switching than an amorphous device, a C-MOS device could achieve a higher frame rate. Characteristics of a C-MOS device are in agreement with the condition required for the detector applied to the dual-energy x-ray CT. It is one of the hopeful candidates.

2.3 Design Parameters of Beamline

In a conventional x-ray CT scanner, the average energy of the x ray is about from 70 to 80 keV. Therefore, it seems reasonable to consider the dual-energy x-ray CT using a 80 keV x ray as the higher energy x ray. It means the energy of the first order harmonic wave is 40 keV. The light source of the beamline is assumed to be the wiggler. The wiggler operated in a maximum magnetic field of 7 T with a 420 mA electron beam of 2.3 GeV produces the flux densities of 3.48×10^{14} (photon/s/mrad^2/0.1% bw) for a 40 keV x ray and 1.27×10^{14} for a 80 keV x ray. The photon emitted horizontally within ±10 mrad is used to make the irradiation field of 300 mm wide. Since an SR beam has a sharp vertical distribution, the photon emitted vertically within only ±0.09 mrad is used to keep the flatness less than ±12.5%. Then, a 2.7 mm high x-ray beam is provided at the monochromator that is located 15 m from the light source. In order to make the irradiation field of 50 mm high, it is necessary to magnify the vertical size 18.5 times. According to Eq. (6), the θ_B of 4.63° for the 40 keV x ray requires the asymmetry angle α to be 4.15° in order to obtain $M=18.5$.

The photon flux of an x ray should be determined according to quality of images and radiation safety. The conventional x-ray CT technique empirically tells us that in order to obtain good quality of images and keep radiation dose within allowance, at least 2.5×10^6 photons per pixel are necessary in the absence of an object. We designed the filter thickness and a way of exposures to roughly keep the empirical rule. Table 1 shows the photon flux and the surface dose in a typical case. The filter consists of (a) a graphite plate with thickness of 13 g/cm^2 and (b) a copper plate of 1.8 g/cm^2. In this calculation, the light source of the beamline is the wiggler with nine poles of 7 T, which is operated in 2.3 GeV 420 mA electron beams. In this case, the exposure time to the x rays for taking a transmission image is assumed to be 0.5 ms each with an interval of 5 ms between both the exposures. The surface dose is much less than 50 mGy, which is an upper limit of an entrance surface dose of a head by x-ray CT scanning recommended by IAEA Basic Safety Standard of 1996.[14]

2.4 Experimental Results on Derivation of ρ_e and Effective Z

The primitive experiment of measurement of attenuation coefficients proved Eqs. (4) and (5) to be effective in deriving electron density and an effective atomic number. The experiment was carried out by using monochromatic x rays of three kinds emitted from radioisotopes of ^{133}Ba and ^{241}Am. Aluminum and four phantoms were used as objects. Three of the phantoms are equivalent to fat, soft tissue and a mixture of a muscle and fat, and the remaining phantom is equivalent to a compact bone. The x rays of 32.2 and 81.0 keV are emitted from ^{133}Ba and the x ray of 59.5 keV is emitted from ^{241}Am. We measured x rays in pulse-height-analysis with an NaI(Tl) crystal scintillator. The detector was well collimated and its

Table 2 Attenuation coefficients measured by monochromatic x rays and derived electron densities and effective atomic numbers. (Note: Electron densities and effective atomic numbers except aluminum target were derived using pairs of data of 32.2 and 81 keV. Those values of aluminum were derived from a pair of data of 32.2 and 59.5 keV.)

	Attenuation coefficients (1/cm)				
Energy (keV)	SZ-202[a]	SZ-207[b]	SZ-49[c]	BET[d]	Aluminum
32.2	0.359	0.340	0.263	1.990	2.444
59.5	0.213	0.211	0.193	0.528	0.734
81	0.192	0.182	0.173	0.378	
$\rho_e(10^{23}/\mathrm{cm}^3)$	3.488	3.319	3.233	5.211	7.629
Exp./Theory	1.038	0.958	0.988	0.968	0.974
Effective Z	7.58	7.56	6.14	13.96	13.08
Exp./Theory	1.06	1.08	1.01	1.06	1.01

[a] SZ-202: Phantom equivalent to mixture of a muscle and fat.

[b] SZ-207: Phantom equivalent to soft tissue.

[c] SZ-49: Phantom equivalent to fat.

[d] BET: Phantom equivalent to compact bone.

solid angle was about 2×10^{-3} strad. Table 2 shows attenuation coefficients of the objects for every energy x ray, effective atomic numbers, and electron densities derived from using Eqs. (4) and (5). The electron densities and effective atomic numbers of the objects except aluminum were derived from using data of 32.3 and 81 keV. For the aluminum object, data of 32.3 and 59.5 keV were used. Discrepancies between the measured values and the theoretical values are less than 5%. Combination of data of 32.3 and 59.5 keV or those of 59.5 and 81 keV, however, leads the discrepancy to being larger than the values shown in Table 2.

3 Design of the Synchrotron Light Source and its Layout

The synchrotron light source shown in Figure 3 was designed to be compact so as to install all the facilities in a limited area such as a hospital. In order to use the light source for clinical purposes, it is necessary to produce sufficient photon flux in a hard x-ray region. Since intravenous CAG in the *K*-edge subtraction technique[1] requires rather high photon flux of 33 keV x ray among other applications, it is expected that the synchrotron light source optimized for the CAG may be applicable to other medical applications, except for the applications using the fluorescent x rays.[15] Therefore, the synchrotron light source proposed here was designed for the CAG.

Electrons are accelerated up to 300 MeV by a linear accelerator at first, then they are injected into a storage ring. The storage ring with a circumference of 80 m stores the electrons with a current of 420 mA or more and accelerates them up to 2.3 GeV. For charged particle beam optical design of the storage ring, a double bend achromat lattice is adaptive in order to set dispersion free at straight sections. There are four straight sections, and two of them are equipped with multipole wigglers. The wiggler has nine poles with spacing of 200 mm and generates a maximum magnetic field of 7 T, which is excited by superconducting coils. One of the wigglers is a light source of the beamline for dual-energy x-ray CT. Another wiggler is used for the beamline designed for the CAG.[16] Energy spectra of the photon radiated from the wiggler and bending magnets are shown in Figure 4. Critical energies of the wiggler operated at 7 T and that of the bending magnet operated at 1.5 T are 24.6 and 5.3 keV, respectively. As shown in the figure, the wiggler can provide sufficient photon flux for a dual-energy x-ray CT scan in the high energy region. The beam emittance is 3.8×10^{-7} mrad during the operation of both the wigglers. Although this value of beam emittance is rather large, it is convenient for making a large irradiation field in a short beamline. The maximum beam size at the straight sections is estimated at $2.4\,\mathrm{mm}\times0.8\,\mathrm{mm}$. Both the beamlines are designed to be about 15 m long from the light sources in order to make the facilities as compact as possible.

4 Discussion

There are many causes such as noise and bad detectors that make a reconstruction image deteriorate. We focus on three of them: (1) rotation in CT scanning, (2) a light source size, and (3) the reflection effect; they seem to relate specifically to the system for the dual-energy x-ray CT.

1. Rotation of an object while taking transmission images makes the spatial resolution poor. As mentioned in Sec. 2.2, two exposures and the interval between them take about 6 ms. During the period, a point in the object rotates about 1 mrad in a rotation rate of 180° per 20 s. This slight rotation makes the point projected on the detector move at most 0.1 mm horizontally. This is much smaller than the horizontal size of a pixel of 1 mm.

2. Since the beamline is short as 15 m, the light source of the beamline cannot be regarded as a point source. In the full power operation mode of the wiggler, the source separates two point sources about 7 mm apart in a deflection plane of

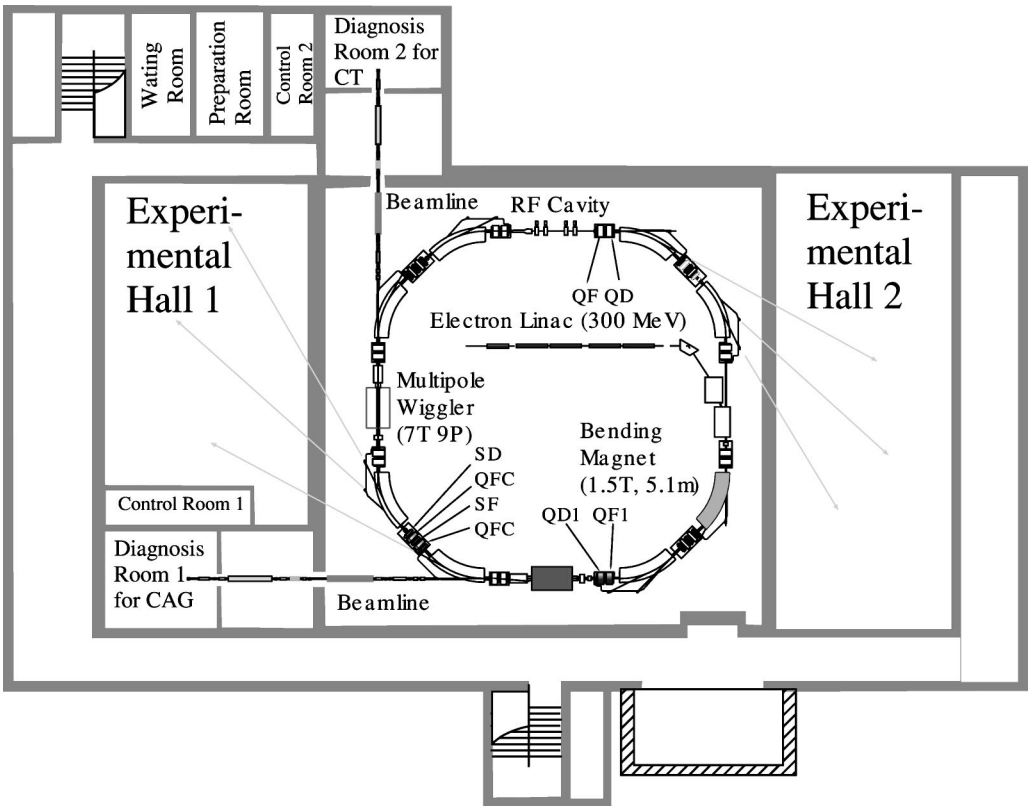

Fig. 3 A layout of the compact synchrotron light source for the medical application is shown. Electrons are injected in the storage ring with 300 MeV from the linear accelerators, and are accelerated up to 2.3 GeV with 420 mA. The storage ring consists of eight bending magnets. There are two superconducting multipole wigglers. Two beamlines of the wigglers are used for diagnoses and a few beamlines of the bending magnets are used for basic research and development of diagnostic techniques.

the electrons in the wiggler magnetic field. The angle between two lines connecting a point of the object and both the sources is 0.5 mrad at maximum. When an object-to-detector distance is 500 mm, each source makes a projected image on the detector. Both the images are 0.2 mm apart, and it is also much shorter than the horizontal size of the pixel.

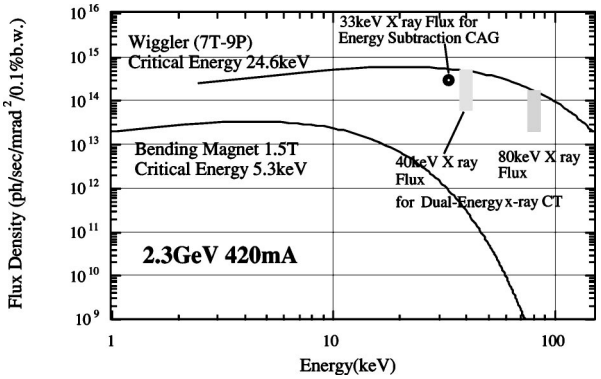

Fig. 4 Spectra of the photon flux produced by the 7 T and nine-pole multipole wiggler and the bending magnet in a mode of 2.3 GeV and 420 mA operation are shown. In the figure, the photon number of 33 keV x ray required for CAG is indicated by a circle. The photon numbers of 40 and 80 keV x rays required for the dual-energy x-ray CT are also indicated by thick bars. The photon numbers required for the CT change according to the filters.

3. Although an effect of refraction, which enhances a boundary of materials with different refractive indices may improve contrast of the image,[17] it could cause us to observe incorrect electron density. Since deflection of a hard x ray in a material is as small as tens of microradians, a short object-to-detector distance enables us to eliminate the enhancement in the image. Besides, the beam emittance of the synchrotron light source designed here is so large that refraction-enhanced images are difficult to make even at a long object-to-detector distance.

Eventually, the effects of 1 and 2 blur the image, but the extent of the deterioration is not so serious: the spatial resolution deteriorates only about 3% in total. The effect of 3 is expected not to affect the image.

Equations (4) and (5) tell us that as the interval between E_1 and E_2 become larger, the resultant ρ_e and Z become more accurate. It has also been shown in the experimental results. In this design, we took E_1 to be 40 keV and E_2 to be 80 keV. From the point of view of photon flux, radiation dose, and energy interval, the selection of the x-ray energy seems to be reasonable.

The design parameters of the filter are key among other parameters. They adjust radiation dose and the ratio of photon flux of the 40 keV x ray to that of the 80 keV x ray. There are only two conditions to select the parameters; (1) radiation dose within allowance, and (2) suitable photon flux ratios. It is easily seen that there is great freedom to select a combination

of materials of the filters and the thickness of them. Different parameters from those mentioned in Sec. 2.3 can decrease the necessary photon flux produced by the light source of the beamline. Then, it affects the design of the light source as well as the design of the beamline. In this sense, the set of parameters mentioned in this paper is only one example. There should be options.

5 Summary

The synchrotron radiation has great potential for medical diagnoses as well as for elemental research and industrial applications. In this paper, we proposed the beamline for the dual-energy x-ray CT as well as the compact synchrotron light source dedicated to the medical applications.

Also, we proposed a method to derive electron density and an effective atomic number from the linear attenuation coefficients measured for two energy x rays. We experimentally proved that the method was effective even for heavy elements such as a bone. Discrepancies of the measured electron density and effective atomic number from the theoretical values are about 5% or less.

The key components of the beamline proposed here are the double crystal monochromator and the rotating filter. They can easily provide two different type x-ray beams one after the other. The beams have the first order harmonic wave and the second order harmonic wave one with a different ratio. Use of the two types of x-ray beams is equivalent to use of two monochromatic x-ray beams with different energies. Combination of the beamline and the iterative method for analyzing the electron density and the effective atomic number can open an avenue to clinical performance of the dual-energy x-ray CT using SR.

The synchrotron light source designed here mainly consists of a compact electron storage ring and two multipole wigglers and beamlines. This design focused on compactness of the total system dedicated to the medical applications such as the energy subtraction CAG and the dual-energy x-ray CT with SR. Since the CAG requires the highest photon flux among the medical applications except for some special applications such as fluorescent x-ray CT,[15] the storage ring and the wiggler were optimized for production of sufficient photon flux for the CAG. Therefore, the facility should be widely applicable to many other diagnoses that need a large amount of photon flux. However, the electron beam emittance is so large that performance of the advanced imaging such as refraction-enhanced imaging and phase-contrast imaging is difficult.

References

1. E. Rubenstein et al., ''Synchrotron radiation and its application to digital subtraction angiography,'' *Proc. SPIE* **34**, 42–49 (1981).
2. S. Ohtsuka, Y. Sugishita, T. Takeda, Y. Itai, J. Tada, K. Hyodo, and M. Ando, ''Dynamic intravenous coronary angiography using 2D monochromatic synchrotron radiation,'' *Br. J. Radiol.* **72**, 24–28 (1999).
3. H. Elleaume et al., ''First human transvenous coronary angiography at the European Synchrotron Radiation Facility,'' *Phys. Med. Biol.* **45**, L39–L43 (2000).
4. W.-R. Dix, T. Dill, C. W. Hamm, M. Jung, W. Kupper, and M. Lohmann, ''Intravenous coronary angiography with synchrotron radiation at HASYLAB,'' *Nucl. Phys. A* **654**, 1043c–1046c (1999).
5. S. Yamada, ''Commissioning and performance of the HIMAC medical accelerator,'' *Proc. of the 1995 IEEE Particle Accelerator Conf.*, pp. 9–13, Dallas, Texas (1995).
6. H. Tsujii et al., ''The current status and perspective of heavy-ion therapy,'' *Proc. of 6th International Meeting on Progress in Radio-Oncology*, pp. 709–721, Salzburg, Austria (May 1998).
7. R. A. Rutherford, B. R. Pullan, and I. Isherwood, ''Measurement of Effective atomic number and electron density using an EMI scanner,'' *Neuroradiology* **11**, 15–21 (1976).
8. E. Nachaliel et al., ''Monochromatic computed tomography of the human brain using synchrotron X-rays: technical feasibility,'' *Nucl. Instrum. Methods Phys. Res. A* **319**, 305–310 (1992).
9. D. F. Jackson and D. J. Hawkes, ''X-Ray attenuation coefficients of elements and mixtures,'' *Phys. Rep.* **70**, 169–233 (1981).
10. K. Kohra, ''An application of asymmetry reflection for obtaining x-ray beams of extremely narrow angular spread,'' *J. Phys. Soc. Jpn.* **17**, 589–590 (1962).
11. A. C. Kak and M. Slaney, ''*Principles of Computerized Tomographic Imaging*,'' p. 77, The Institute of Electrical and Electronics Engineers, Inc., New York (1988).
12. M. J. Yaffe and J. A. Rowlands, ''X-ray detectors for digital radiography,'' *Phys. Med. Biol.* **42**, 1–39 (1997).
13. K. Nakagawa, Y. Aoki, Y. Sasaki, A. Akanuma, and S. Mizuno, ''C-MOS flat-panel sensor for real time x-ray imaging,'' *Nippon Acta Radiol.* **58**, 81–85 (1998) (Japanese).
14. IAEA, ''International Basic Safety Standards for Protection against Ionizing Radiation and for the Safety of Radiation Sources,'' Safety Series No. 115 (1996).
15. T. Takeda, T. Maeda, T. Yuasa, T. Akatsuka, T. Ito, K. Kishi, J. Wu, M. Kazama, K. Hyodo, and Y. Itai, ''Fluorescent scanning x-ray tomography with synchrotron radiation,'' *Rev. Sci. Instrum.* **66**, 1471–1473 (1995).
16. M. Torikoshi, M. Endo, M. Kumada, K. Noda, S. Yamada, and K. Kawachi, ''Design of a compact synchrotron light source for medical applications at NIRS,'' *J. Synchrotron Radiat.* **5**, 336–338 (1998).
17. N. Yagi, Y. Suzuki, K. Umetani, Y. Kohmura, and K. Yamazaki, ''Refraction-enhanced x-ray imaging of mouse lung using synchrotron radiation source,'' *Med. Phys.* **26**, 2190–2193 (1999).